



Synthesis and evaluation of pyrazolo[1,5-b]pyridazines as selective cyclin dependent kinase inhibitors

Kirk L. Stevens^{a,*}, Michael J. Reno^a, Jennifer B. Alberti^a, Daniel J. Price^b, Laurie S. Kane-Carson^c, Victoria B. Knick^d, Lisa M. Shewchuk^b, Anne M. Hassell^b, James M. Veal^{a,†}, Stephen T. Davis^{d,‡}, Robert J. Griffin^e, Michael R. Peel^{a,§}

^a Department of Oncology, Medicinal Chemistry, GlaxoSmithKline, Research Triangle Park, NC 27709, USA

^b Department of Computational and Structural Chemistry, GlaxoSmithKline, Research Triangle Park, NC 27709, USA

^c Department of Molecular Biochemistry, GlaxoSmithKline, Research Triangle Park, NC 27709, USA

^d Department of Cancer Biology, GlaxoSmithKline, Research Triangle Park, NC 27709, USA

^e Department of Drug Metabolism and Pharmacokinetics, GlaxoSmithKline, Research Triangle Park, NC 27709, USA

ARTICLE INFO

Article history:

Received 8 September 2008

Revised 16 September 2008

Accepted 19 September 2008

Available online 24 September 2008

Keywords:

Cyclin-dependant kinase inhibitor

CDK2

CDK4

VEGFR-2

GSK3 β

Pyrazolo[1,5-b] pyridazine

Cancer

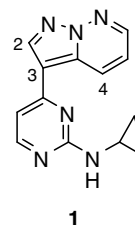
ABSTRACT

A novel series of pyrazolo[1,5-b]pyridazines have been synthesized and identified as cyclin dependant kinase inhibitors potentially useful for the treatment of solid tumors. Modification of the hinge-binding amine or the C(2)- and C(6)-substitutions on the pyrazolopyridazine core provided potent inhibitors of CDK4 and demonstrated enzyme selectivity against VEGFR-2 and GSK3 β .

© 2008 Elsevier Ltd. All rights reserved.

The current treatments for cancer have a highly fragmented market since these agents are only active in specific patient populations or tumor types. The accumulation of genetic and biological information from solid tumors is providing additional targets that have the potential of yielding drugs with broad activity and less toxicity than current therapies. Human genetic evidence supports the cyclin dependant kinase (CDK) family as key therapeutic targets for disease modification. In particular, the cyclin D/CDK4/pRb tumor suppressor pathway of cell growth control is frequently deregulated in human cancers.¹ Several lines of evidence suggest that perturbation of this pathway is on the critical path toward tumorigenesis.² The CDK4 pathway of cell growth control is frequently altered by overexpression of cyclin D1, the activation sub-unit of CDK4, in breast, lung, and pancreatic cancers.³ Also, antisense RNA to cyclin D1 sensitizes tumor cells to chemotherapy⁴ and cyclin D1 overexpression correlates with poor disease

outcome.⁵ An estimated 60–70% of human cancers including breast, non-small cell lung, and colon cancer are pRb positive and could respond to selective inhibition of CDK4.⁶



Following a screening campaign on CDK4 and subsequent cross-screening of hits against a panel of kinases, pyrazolopyridazine **1** was identified as having compelling CDK family activity, being roughly equipotent on the 3 isoforms screened at approximately 100 nM.⁷ Screening hit **1** was attractive in that, despite its relatively modest molecular weight (252 amu), it was >100-fold selective over

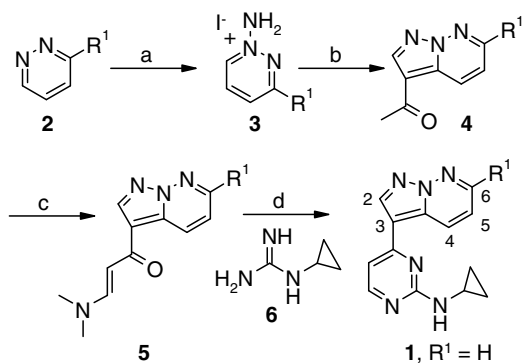
* Corresponding author. Tel.: +1 919 483 7707; fax: +1 919 483 6053.

E-mail address: Kirk.L.Stevens@gsk.com (K.L. Stevens).

[†] Present address: Serenex Inc., Durham, NC, USA.

[‡] Present address: TransTech Pharma Inc., High Point, NC, USA.

[§] Present address: Scynexis Inc., Durham, NC, USA.



Scheme 1. Reagents and conditions: (a) HOSA, KHCO_3 , KI, H_2O (use product without purification); (b) butyn-2-one, KOH, $\text{CH}_2\text{Cl}_2/\text{H}_2\text{O}$, (80–90%); (c) DMF/DMA (75–90%); (d) K_2CO_3 , **6**, DMF (55–77%).

12 of the 18 non-CDK family kinases screened and ~ 10 -fold selective over the rest. However, developability profiling determined **1** suffered from high intrinsic clearance as measured by stability in mouse liver S9 fractions. To be considered a good starting point for the program, it was necessary to demonstrate that the scaffold had the capacity for improved potency, CDK2 selectivity, and metabolic stability. A preliminary synthetic chemistry effort was mobilized to determine if improvements in these properties were achievable among close analogs.

Pyrazolopyridazines were prepared in an efficient manner by initial reaction of pyridazines (**2**) with hydroxyl amine sulfonic acid (HOSA) to afford the aminated pyridazines (**3**, Scheme 1). This was followed by a formal [3+2] cycloaddition between the desired 1-amino-pyridazines and butyn-2-one under basic conditions to give pyrazolo[1,5-b]pyridazines (**4**). Condensation with DMF/DMA afforded enamines (**5**), which gave the corresponding pyrimidine **1** upon exposure to guanidine (**6**) under basic conditions at elevated temperatures.⁸

With an efficient synthesis in hand, we focused our attention on optimizing kinase potency and selectivity. A crystal structure of **1** bound to the kinase domain of human CDK2 was obtained (Fig. 1).^{9,10}

CDK4 is very difficult to express and purify and, to our knowledge, there are no CDK4 structures in the literature. Therefore, CDK2 was utilized as a surrogate for CDK4 due to the close homology within the active site and based on information gathered from ongoing efforts with CDK2.¹¹ The crystal structure revealed that the amino-pyrimidine acts as a two-point hydrogen-bond donor/

acceptor pair to the hinge region of the ATP binding site and the pyrazolopyridazine presents its extended electronegative edge to the catalytic lysine. Subsequent crystal structures of compounds within the series complexed with CDK2 suggested the binding mode was invariant to the substitutions discussed here. To affect CDK4 potency, we targeted three areas of the of the ATP binding pocket that historically have improved potency in other kinases: (1) the inner hydrophobic area near the phenylalanine gatekeeper, (2) the hydrophobic pocket beneath the G-rich loop, and (3) the hinge/solvent exposed area.^{12,13}

Our crystal structure suggested that the space near the gatekeeper was accessible from the 2-position of the pyrazolopyridazine. The CDK family of kinases possesses a sterically imposing phenylalanine gatekeeper that was expected to be unaccommodating to larger substituents. Indeed, compounds were prepared which verified that even a methyl group lowers CDK4 activity 5- to 10-fold (Table 1, **7** and **11**).¹⁴ This trend is in stark contrast to VEGFR-2, which contains a more permissive valine gatekeeper and sees increasing activity with increasingly large substitutions at this position (Table 1, **7–9**, **11–13**).

Crystallography also suggested that adding bulk either directly at the 6-position or with a 1-atom linker would access the area under the G-rich loop. In order to affect substitution at the 6-position we needed a synthetic handle. We envisioned a cross coupling reaction or direct displacement of a halogen. Since we did not expect a halogen to survive the cycloaddition chemistry to **4**, due to displacement by water, we used a methoxy group on the pyridazine (Schemes 1 and 2, $\text{R}^1 = \text{OMe}$) which we expected could be converted to a leaving group for subsequent chemistry. Standard demethylation conditions using mineral acids with heating on **4** or **1** gave only moderate conversion to the respective hydroxyl compounds in about 50% isolated yield. Therefore, alternative chemistry was developed to convert this methoxy group to a cross coupling partner or appropriate leaving group. Nucleophilic conditions using morpholine for deprotection proved to be the most efficient and highest yielding (**14**, Scheme 2) providing the pyrazolopyridazinone in 85–90% yield.¹⁵ We converted this compound to the triflate utilizing *N*-phenyl triflimide in 75–85% yield. We found the triflate leaving group to be more effective than conversion to a halogen in the subsequent displacement reactions to prepare amine substitutions (**16**) or as a cross coupling partner to prepare aryl or vinyl substitutions (**17**).

Unfortunately, improvement of CDK4 potency was not achieved with these substitutions (Table 2); however, there are notable kinase selectivity trends. Specifically, GSK3 β is less tolerant of bulk at this position. Even a two carbon vinyl substitution (**17**) reduces GSK3 β enzyme potency as compared to **1**. Anything larger, such as a cycloalkyl (**16**), an aryl or heteroaryl (**18**, **19**), or heteroalkyl (**20**) removes measurable GSK3 β activity (Table 2). Electronic factors are also involved as all oxygen linked substituents had reduced potency (**14**, **22**, **23**).

We considered a structural rationale for the selectivity of compounds **16–23**. One publicly available crystal structure of GSK3 β (pdb code 1O9U) aligns well with our internal crystal structures bound to a variety of ligands.¹⁶ These structures show Phe67 extended down, and tucked under, the G-rich loop, thereby occupying the same space accessible from the 6-position of the pyrazolopyridazine. Admittedly, there are multiple publicly available crystal structures of ligand-bound GSK3 β showing Phe67 in a variety of positions, however it is unclear from static structures the relative stability of these conformations. It is postulated here that CDK-family kinases, which have a tyrosine at this position (Tyr17 in CDK4 and Tyr15 in CDK2), more stably adopt this Phe/Tyr 'out' conformation that would be necessary to accommodate a 6-substituent by directly coordinating the catalytic lysine and the proximal conserved glutamate (Lys33 and Glu51 in CDK2).

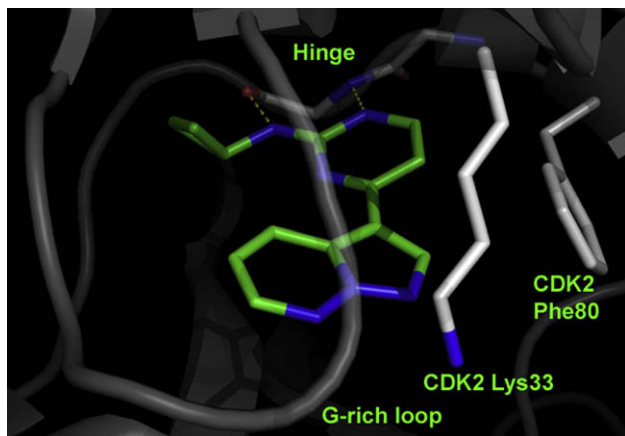
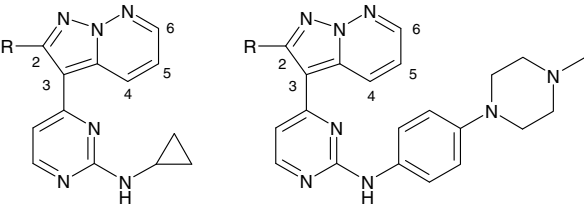


Figure 1. CDK2 crystal structure of **1** showing interaction of the pyrazolopyridazine with catalytic lysine and phenylalanine gatekeeper.

Table 1

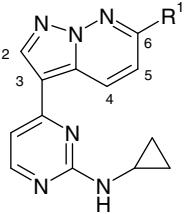
Comparison of CDK4 and VEGFR-2 enzyme potency



R	Compound #	CDK4 IC ₅₀ ^a (μM)	VEGFR-2 IC ₅₀ ^a (μM)	Compound #	CDK4 IC ₅₀ ^a (μM)	VEGFR-2 IC ₅₀ ^a (μM)
H	1	0.080	>20	10	0.012	0.400
Methyl	7	0.800	>20	11	0.050	0.063
Ethyl	8	2.00	3.2	12	0.025	0.063
<i>n</i> -Butyl	9	>40	2.5	13	0.800	0.025

^a Values are the mean of two or more experiments.**Table 2**

CDK4 and GSK3β enzyme activity—6-position substitutions



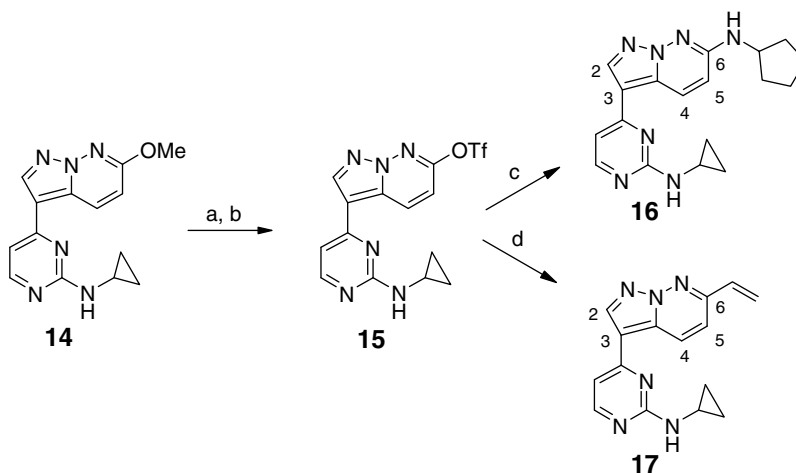
Compound #	R ¹	CDK4 IC ₅₀ ^a (μM)	GSK3β IC ₅₀ ^a (μM)
1	H	0.080	1.600
14	–OCH ₃	2.00	25
16	–NH–Cyclopentyl	0.160	25
17	–CH=CH ₂	0.200	3.2
18	2-Thiophene	0.250	>32
19	<i>p</i> -Fluorophenyl	0.250	>32
20	<i>N</i> -morpholine	0.400	25
21	Pyrrolidine	0.500	25
22	–OH	1.30	25
23	–O–Isopropyl	1.60	25

^a Values are the mean of two or more experiments.

Figure 2 shows the overlay of a ‘Phe-in’ GSK3β structure with the ‘Tyr-out’ conformation observed with compound **41** bound to CDK2.¹⁰

It is known that many kinases prefer an aromatic group along the hinge,¹² as opposed to the cyclopropylamino substitution at the 2-position of the pyrimidine as described. Indeed, potency is improved by replacing the cyclopropylamine with a substituted aniline, however, it also significantly erodes the selectivity against other kinases, such as GSK3β (Table 3, **27–34**). Alkyl amino substituents other than cyclopropyl made poor CDK4 inhibitors (Table 3, **24–26**). Aniline substituents had a wide variety of effects on the CDK activity and selectivity. The *para*-*N*-methylpiperazine aniline substitution (Table 3, **10**) gave moderate CDK2 selectivity (~8×) however addition of an additional *meta*-substituent resulted in loss of CDK2 selectivity (Table 3, **28**). While several extremely potent *meta*- and *para*-substituted anilines were identified (Table 3, **30–34**), highlighting the scaffold’s capacity for high CDK4 potency, they also had less desirable selectivity against both CDK-family members and other kinases.

Selectivity over CDK2 at the expense of broader kinase inhibition profile is not an acceptable profile for a CDK4 inhibitor. However, the selectivity trends we observed suggested that proper combinations of substitutions on the template could be expected to reassert the selectivity over GSK3β while maintaining CDK2



Scheme 2. Reagents and conditions: (a) morpholine, 90 °C, 24 h (85–90%); (b) NaH, Tf₂NPh, DMF (75–85%) (c) DIEA, cyclopentylamine, DMF (66%); (d) vinyltributylstannane, Pd₂(dba)₃, DMF (55%).

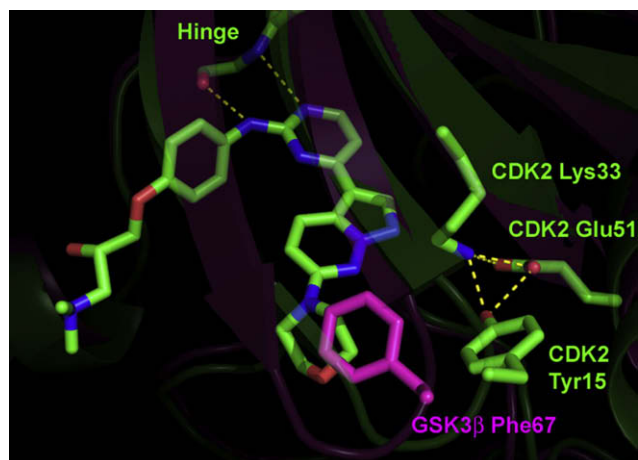
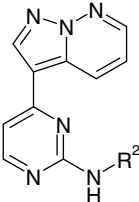
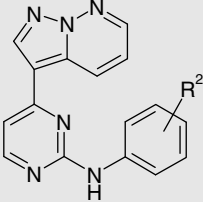


Figure 2. CDK2 crystal structure with (**41**) (green) and overlay with 'Phe-in' (pink) of GSK3β (pdb code 1O9U). GSK3β ligand and all residues except Phe67/Tyr15 removed for clarity.

Table 3
CDK4, CDK2, and GSK3β enzyme activity—substitution at R²



Compound #	R ²	CDK4 IC ₅₀ ^a (μM)	CDK2 IC ₅₀ ^a (μM)	GSK3β IC ₅₀ ^a (μM)
1	–Cyclopropyl	0.080	0.120	1.600
24	–CH ₂ CF ₃	1.00	1.00	>32
25	–CH ₂ –(<i>p</i> -chlorophenyl)	1.00	1.00	10
26	–CH ₂ CH ₂ CH ₂ –(<i>N</i> -morpholine)	3.20	NA	32

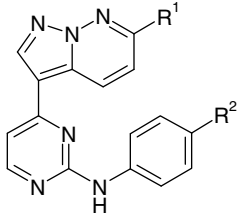


Compound #	R ²	CDK4 IC ₅₀ ^a (μM)	CDK2 IC ₅₀ ^a (μM)	GSK3β IC ₅₀ ^a (μM)
27	H	0.012	0.008	0.032
10	<i>p</i> –(<i>N</i> -methyl)- <i>N</i> -piperazine	0.012	0.100	0.200
28	<i>m</i> –CF ₃ , <i>p</i> –(<i>N</i> -methyl piperazine)	0.006	0.004	0.016
29	<i>m</i> –CH ₂ N(CH ₂ CH ₃) ₂	0.012	0.050	0.079
30	<i>p</i> –NO ₂	0.008	0.003	0.005
31	<i>m</i> –NO ₂	0.0003	0.0003	0.002
32	<i>p</i> –CN	0.025	0.002	0.005
33	<i>m</i> –CN	0.004	0.002	0.010
34	<i>m</i> –(4-oxazolyl)	0.016	0.003	0.008
35	<i>p</i> –CONH ₂	0.160	0.016	0.020
36	<i>p</i> –CO ₂ H	0.790	0.040	0.050
37	<i>p</i> –Isopropyl	2.000	0.040	0.016
38	<i>m</i> –CONHCH ₂ CH ₂ N(CH ₂ CH ₃) ₂	0.008	0.040	0.020

^a Values are the mean of two or more experiments.

selectivity, for example, by using *p*-fluorophenyl at R¹ and 1-methyl-4-phenyl piperazine at R² (from compounds **19** and **10**,

Table 4
CDK4 and GSK3β enzyme activity—double substituted analogs



Compound #	R ¹	R ²	CDK4 IC ₅₀ ^a (μM)	CDK2 IC ₅₀ ^a (μM)	GSK3β IC ₅₀ ^a (μM)
1	H	NA, cyclopropylamine	0.080	0.120	1.600
10	H	<i>p</i> –(<i>N</i> -methyl)- <i>N</i> -piperazine	0.012	0.100	0.200
39	<i>p</i> –F-Phenyl–	<i>p</i> –(<i>N</i> -methyl)- <i>N</i> -piperazine	0.026	0.740	>25
40	–O–Isopropyl	<i>p</i> –(<i>N</i> -methyl)- <i>N</i> -piperazine	0.045	0.230	0.850
41	–Morpholine	<i>p</i> –(<i>N</i> -methyl)- <i>N</i> -piperazine	0.038	0.450	0.690

^a Values are the mean of two or more experiments.

respectively). **Table 4** illustrates select analogs with substituted anilino hinge-binders crossed with 6-position substitutions that achieve both selectivity goals. Compound **39** (CDK4 IC₅₀ = 26 nM) highlights this effort, achieving >10-fold CDK2 selectivity and >100-fold GSK3β selectivity.

The majority of the compounds described were profiled for metabolic stability in mouse liver S9 fractions. While modest improvements were seen for some anilines and some 6-substitutions relative to the original hit (**1**), most compounds profiled showed more than 85% turnover after 60-min incubation in mouse liver S9 fractions. As expected from the high turnover, representative examples did not show acceptable oral exposure in mice. Compounds **20** and **23** had dose normalized AUC > 1000 ng h/mL/mg/kg. While the morpholine and –O-*iso*-propyl derivatives were the best of the cyclopropylamine-substituted series, this trend did not hold for the *p*–(*N*-methyl)-*N*-piperazine aniline series. Compound **41**,¹⁷ however, represented an improvement in turnover in mouse liver S9 fractions (46% after 60-min incubation). This compound also demonstrated acceptable selectivity over CDK2 and GSK3β, although it failed to achieve any oral exposure. Compound **41** displayed much greater exposure when delivered *i.p.* (DNAUC > 7000 ng h/mL/mg/kg) suggesting that poor adsorption rather than metabolism is most likely the cause of poor oral exposure.

In summary, a flexible, efficient synthesis was used to prepare analogs which varied at the 6-position of the pyrazolopyridazine and the amine on the pyrimidine hinge binder. Based on X-ray studies, analogs were prepared which improved or maintained CDK4 enzyme activity while improving kinase selectivity over VEGFR-2 and GSK3β. With limited, iterative chemistry, analogs were quickly identified that demonstrated the pyrazolopyridazine template's capacity for acceptable CDK2 selectivity and improved metabolic stability. Further lead optimization details will be reported in a subsequent communication.

References and notes

- Valentini, A.; Gravina, P.; Federici, G.; Bernardini, S. *Cancer Biol. Ther.* **2007**, *62*, 185.
- Bartkova, J.; Lukas, J.; Guldberg, P.; Alsner, J.; Kirkin, A.; Zeuthen, J.; Bartek, J. *Cancer Res.* **1996**, *56*, 5475.
- (a) Reissmann, P. T.; Koga, H.; Figlin, R. A.; Holmes, E. C.; Slamon, D. J. *J. Cancer Res. Clin. Oncol.* **1999**, *1252*, 61; (b) Gillett, C.; Fantl, V.; Smith, R.; Fisher, C.; Bartek, J.; Dickson, C.; Barnes, D.; Peters, G. *Cancer Res.* **1994**, *547*, 1812; (c) Motokura, T.; Arnold, A. *Curr. Opin. Genet. Dev.* **1993**, *31*, 5; (d) Arber, N.; Gammon, M. D.; Hibshoosh, H.; Britton, J. A.; Zhang, Y.; Schonberg, J. B.; Rotterdam, H.; Fabian, I.; Holt, P. R.; Weinstein, I. B. *Hum. Pathol.* **1999**, *309*, 1087.
- Kornmann, M.; Danenberg, K. D.; Arber, N.; Beger, H. G.; Danenberg, P. V.; Korc, M. *Cancer Res.* **1999**, *5914*, 3505.
- Hosokawa, Y.; Andrew, A. *Genes Chromosom. Cancer* **1998**, *221*, 66.
- (a) Fokkema, E.; Timens, W.; de Vries, E. G. E.; de Jong, S.; Fidler, V.; Meijer, C.; Groen, H. J. M. *Lung Cancer* **2006**, *522*, 241; (b) Ali, A. A.; Marcus, J. N.; Harvey, J. P.; Roll, R.; Hodgson, C. P.; Wildrick, D. M.; Chakraborty, A.; Boman, B. M. *FASEB J.* **1993**, *7*, 931.
- Pyrazolo[1,5-b]pyridazines have been used as 5HT₃-antagonists, Cox 2 inhibitors, and GSK-3 β inhibitors (a) Bondo, H. J.; Weis, J.; Suzdak, P. D.; Eskesen, K. *Bioorg. Med. Chem. Lett.* **1994**, *45*, 695; (b) Beswick, P.; Bingham, S.; Bountra, C.; Brown, T.; Browning, K.; Campbell, I.; Chessell, I.; Clayton, N.; Collins, S.; Corfield, J.; Guntrip, S.; Haslam, C.; Lambeth, P.; Lucas, F.; Mathews, N.; Murkit, G.; Naylor, A.; Pegg, N.; Pickup, E.; Player, H.; Price, H.; Stevens, A.; Stratton, S.; Wiseman, J. *Bioorg. Med. Chem. Lett.* **2004**, *5445*; (c) Liu, L.; Zhang, L.; Jiang, F.-C. *Chin. J. Chem.* **2007**, *257*, 892.
- For full experimental details and spectral data on the preparation of pyrazolopyridazines, please see: Harris, P.; Jung, D.; Peel, M.; Reno, M.; Rheault, T.; Stanford, J.; Stevens, K.; Veal, J. *PCT Int. Appl.* **2003**, *134*, WO 0351886.
- The expression, purification and crystallization of CDK-2/Cyclin A was carried out as previously described Jeffrey, P. D.; Russo, A. A.; Polyak, K.; Gibbs, E.; Hurwitz, J.; Massagué, J.; Pavletich, N. P. *Nature* **1995**, *376*, 313. Crystals were soaked with 50 μ M compound for 2 days prior to data collections. The structures were refined to an Rfactor of 21% at 3.0 Å. The PDB deposition codes for the structures are 3EID and XXXX.
- Image generated with PyMol (Delano Scientific).
- (a) Thomas, M. P.; McInnes, C.; Fischer, P. M. *J. Med. Chem.* **2006**, *491*, 92; (b) Park, K.-S.; Kim, J.; Chong, Y.; Choo, H. *Bull. Korean Chem. Soc.* **2007**, *282*, 211; (c) Vadivelan, S.; Sinha, B.; Irudayam, S.; Jagarlapudi, S. A. R. P. *J. Chem. Inf. Model.* **2007**, *47*, 1526.
- Aronov, A.; Murcko, M. J. *Med. Chem.* **2004**, *47*, 5616.
- Davies, T. G.; Pratt, D. J.; Endicott, J. A.; Johnson, L. N.; Noble, M. E. M. *Pharmacol. Ther.* **2002**, *93*, 125.
- Radioactive Glutathione plate-binding assay of CDK4.** Fifty microliters of reaction mixtures, containing 100 mM HEPES, pH 7.5, 0.5 μ M GST-RB protein, 1 μ Ci/mL [γ -³²P]ATP, 10 mM MgCl₂, 2.5 mM EDTA, 0.2 mg/mL BSA, 1 mM DTT and 7.5 nM CDK4/cyclinD1 enzyme, were prepared in polystyrene plates. The reactions were started by addition of enzyme and quenched after 20–30 min of incubation by addition of 50 μ L 100 mM EDTA, pH 8.0, 2 mM ATP. 100 μ L of each quenched reaction mixture was transferred to a glutathione-coated plate, and incubated at rt (22 °C) overnight. The glutathione-coated plate was then washed with a plate washer with 4 \times 150 μ L/well de-ionized H₂O. Following washing, 150 μ L/well Ultima-Flo M scintillant was added. The radioactivity of each well of the plate was then determined in a micro- β plate counter. **HTRF assay of VEGFR2.** Sixty microliters of reaction mixtures, containing 10 nM VEGFR-2 enzyme, 0.1 M HEPES, pH 7.5, 0.1 mg/mL BSA, 1 mM DTT, 360 nM peptide (biotin-aminohexyl-EEEEYFELVAKKKK-NH₂), 75 μ M ATP, and 5 mM MgCl₂, were prepared in polystyrene plates. The reactions were started by addition of enzyme to substrate and quenched after 40–60 min of rt incubation by addition of 40 μ L 100 mM EDTA, pH 8.0 in 0.1 M HEPES. 50 μ L of HTRF reagents were added and incubated for a minimum of 10 min. The fluorescence was then measured at 665 nm on a Victor plate reader using a time delay of 50 μ s. **SPA assay of GSK3 β .** Thirty microliters reaction mixtures containing, 1.13 μ M peptide, 100 mM HEPES, pH 7.2, 10 mM MgCl₂, 0.3 mg/mL heparin, 0.1 mg/mL BSA, 1 mM DTT, 2.5 μ M ATP, 0.0066 Ci/ μ L ³²P-ATP, and 1.2 μ g/mL GSK3 β protein were prepared in polystyrene plates. The reactions were started by addition of enzyme to substrate and were terminated by addition of 20 μ L of stop solution [0.25 M EDTA, pH 8, 2.5 mM unlabelled ATP]. 195 μ L of 1.3 mg/mL StreptAvidin-coated SPA beads in PBS were added and the plates counted in a Packard TopCount (1 min/well) after 10 h.
- Although we elucidated the demethylation conditions independently, there are examples of using morpholine for demethylations (a) Goclik, V.; Mischnick, P. *Carbohydr. Res.* **2003**, *338*, 733; (b) Bennett, G. J.; Lee, H.-H. *Tetrahedron Lett.* **1989**, *30*, 51, 7265.
- Dajani, R.; Fraser, E.; Roe, S. M.; Yeo, M.; Good, V.; Thompson, V.; Dale, T. C.; Pearl, L. H. *EMBO J.* **2003**, *22*, 494.
- The aniline was suggested from Breault, G. A.; Ellston, R. P. A.; Green, S.; James, S. R.; Jewsbury, P. J.; Midgley, C. J.; Pauptit, R. A.; Minshull, C. A.; Tucker, J. A.; Pease, J. E. *Bioorg. Med. Chem. Lett.* **2003**, *1318*, 2961.